Quart. J. R. Met. Soc. (1984), **110**, pp. 633–656 551.465.71

Solar heating of the oceans—diurnal, seasonal and meridional variation

By J. D. WOODS, W. BARKMANN and A. HORCH
Institut für Meereskunde an der Universität Kiel

(Received 24 May 1983; revised 3 January 1984)

SUMMARY

Solar heating is an important factor in modelling the upper boundary layer of the ocean. It influences not only the temperature, but also the depth of the mixed layer and must be taken into account in circulation dynamics. The study reported in this paper was designed to reveal the principal features of the global climatology of solar heating in the ocean, with such applications in mind. The meridional, seasonal and diurnal variations of the vertical distribution of solar heating inside the ocean, expressed in terms of $I(z)$, the rate of heat accumulation below depth z, and $\dot{T}(z) = (1/c) \cdot d_z I(z)$, the rate of temperature rise, are calculated for given values of cloud cover and seawater turbidity (expressed in terms of Jerlov's water types) using a model that incorporates a new parametrization of $I(z)/I(0)$, which is shown to be more accurate than previous versions. At present there exist no reliable global climatologies of cloud cover and seawater turbidity, so the values of the corresponding parameters are held constant in each computation, which is then repeated using parameter sets covering the full ranges from clear to overcast sky, clear to turbid ocean water. It is found that uncertainty in cloud cover is more important in the mixed layer, and uncertainty in seawater turbidity is more important below. The results presented in this paper are mainly concerned with solar heating below the mixed layer. It is calculated that the annual temperature rise can exceed 1 K and the annual heat accumulation can exceed 100 MJ/m^2 below the mixed layer in the tropics. At higher latitudes solar heating produces similar heating rates in summer, but the stored heat is extracted locally in winter when the mixed layer depth exceeds the maximum depth of solar heating, defined here by a daily temperature rise of 1 mK or a heat flux of 86·4 KJ/m^{2}d (=1 W/m^2). The sensitivity of the seasonal and meridional variations of the maximum depth of solar heating to cloud cover and seawater turbidity is investigated. The actual change of temperature due to solar heating in the seasonal thermocline at Ocean Weather Station 'C' is calculated using Bunker's monthly mean cloud cover and Jerlov's seawater turbidity. Extension of such calculations to the whole of the World Ocean must await the publication of global climatologies of cloud cover and seawater turbidity, which are expected to be derived from satellite observations during the next decade.

A solar heating climatology is a prerequisite for computation of the thermal response of the ocean to CO_2 pollution of the atmosphere. The implications of the results obtained from the present study are discussed. An early rise in tropical sea surface temperature seems likely, but exact prediction will be hindered by uncertainty in the turbidity of the tropical ocean.

1. INTRODUCTION

More than half of the solar energy flux driving the global climate system is first absorbed inside the ocean. It is absorbed over a depth range that exceeds the global mean depth of the ocean mixed layer. Solar heating near the surface is so intense that it quenches convection and turbulence, giving a large diurnal change in mixed layer depth (Woods 1980). The vertical distribution of solar heating is therefore an important factor in modelling upper ocean mixing. Heating below the mixed layer is weak, but can be significant on longer time scales; for example, in the thermal response of the ocean to carbon dioxide pollution of the atmosphere. Ramanathan (1981) has shown that the effect of doubling the atmospheric CO_2 concentration is to change the surface net infrared flux by 100 MJ/m^{2}y. All terms in the global heat budget, including solar heating, must be calculated to an accuracy of, say, 10% of that value. It is, therefore, appropriate to take 10 MJ/m^{2}y as one criterion for the maximum depth of solar heating. It will be shown that over half of the World Ocean (in the tropics) the mixed layer never gets as deep as that solar heating limit; some of the energy supply to the climate system must first be advected to regions of upwelling or to higher latitudes, before it enters the mixed layer, where it is displaced by Ekman flow and can escape to the atmosphere. The fact that the absorption of solar energy extends to a considerable depth in the ocean introduces a delay before the heat can escape to the atmosphere, allowing 1% of the energy throughput to be transported global distances by the ocean currents, an important factor in the energy budget of the climate system (Oort and Vonder Haar 1976).

Those preliminary remarks were intended to prepare the reader for the idea that we need a global climatology of the depth distribution of solar heating in the ocean, giving its regional and seasonal variation. At present no such climatology exists and, as we shall see later, the global data needed to construct one are not yet available. Nevertheless, it is possible to gain some insight into the likely characteristics of such a climatology by making assumptions about the relevant variables, and by undertaking sensitivity tests with them. That is the purpose of the study reported in this paper. It serves as an introduction to the problem, and establishes some useful limits.

2. The scientific problem

The vertical distribution of solar heating is proportional to the divergence of the vertical flux of solar energy, $I(z)$, also called the solar irradiance:

$$\dot{T}(z) = d_t T(z) = (1/c).d_z I(z), \tag{1}$$

where the specific heat of seawater, $c \doteq 4{\cdot}1\ \mathrm{MJ/m^3K}$; so a solar energy flux divergence of $1\ \mathrm{W/m^3}$ raises the temperature by nearly 1 mK/h. (Note that throughout this paper we are concerned solely with the contribution of solar heating to temperature change: other contributions, such as surface cooling and vertical mixing, are not included here.)

Jerlov (1976) and Paulson (1980) have reviewed methods of measuring the vertical profile of solar irradiance. It is a slow and difficult procedure whose accuracy is limited by instrument error to about 2% and involving practical problems of shadowing by the platform from which the instrument is lowered. These difficulties increase sharply when the instrument enters the surface wave zone; with the result that few data are available in the top metre of the ocean. Deeper than one metre, $I(z)$ can be measured with sufficient accuracy for present day climatological purposes. But the number of such profiles is very small, and quite insufficient as a data base for an empirical climatology of solar heating.

It is therefore necessary to adopt the alternative strategy of constructing a climatology on the basis of a model of solar heating, tuned to the few available measurements. The design of such a model has been discussed in the scientific literature by a number of authors in recent years (e.g. Ivanoff 1977). The principal ingredients (see Fig. 1) can be divided into three groups.

Group 1: Calculation of the solar energy flux $I'(0)$ at the bottom of the atmosphere from atmospheric variables, including clouds, dust, water vapour, air.

Group 2: Calculation of the surface albedo, $A = (1 - I(0)/I'(0))$, where $I(0)$ is the energy flux at the top of the ocean, from the angular incidence of $I'(0)$ and the spectrum of surface waves.

Group 3: Calculation of the vertical distribution of solar irradiance inside the ocean, $I(z)$, and hence the heating rate, $\dot{T}(z)$, from oceanic variables, including absorption and scattering by water molecules and particles (especially plankton).

The atmospheric group (1) has been discussed extensively in the meteorological literature (e.g. Kondratyev 1969; Paltridge and Platt 1976). Methods of measuring $I'(0)$ *in situ* at sea, and some recent results, have been reviewed by Simpson and Paulson (1979) and Hinzpeter (1980). The number of such measurements is too small for an empirical global climatology. Gautier *et al.* (1980) have developed a model to calculate $I'(0)$ from satellite observations, and Gautier (1982a) has shown that the results agree with ship measurements of $I'(0)$ made during GATE, to within $\pm 17\ \mathrm{W/m^2}$. In a later paper Gautier (1982b) used the model to map $I'(0)$ over the ocean for 10-day periods

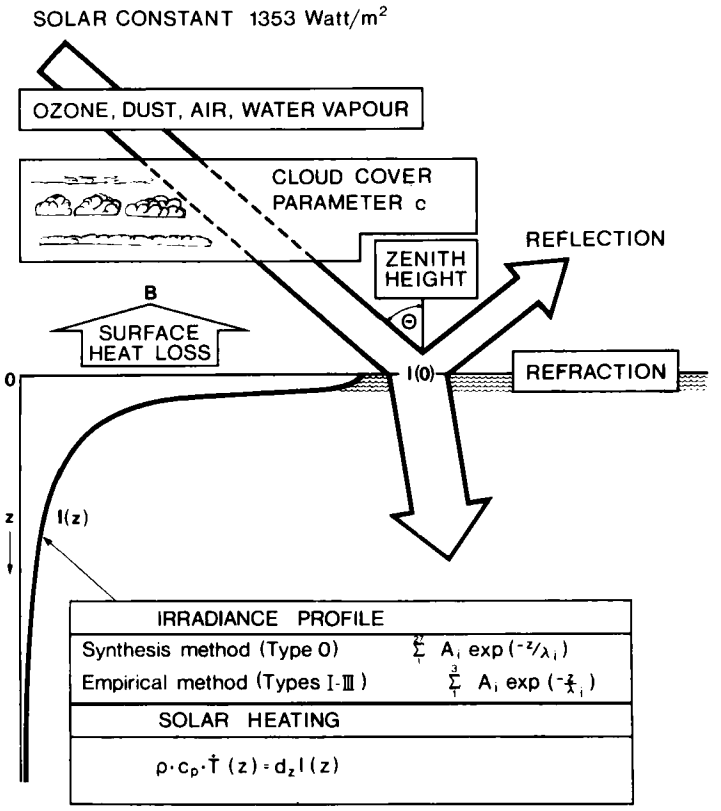

Figure 1. Schematic of the solar heating model used in this study.

during the Global Weather Experiment (1979). The atmospheric variables needed to calculate $I'(0)$ can also be derived from a model in which clouds, water vapour, etc are free variables. Charlock (1982) has discussed simple coupled ocean–atmosphere models in which that is done. $I'(0)$ can also, of course, be extracted as a routine product of the large global models of atmospheric circulation, but we are not aware of any publication comparing such products with *in situ* measurements.

Turning to group 2, Payne (1972) has discussed the ocean surface albedo in detail. The mean value is small (about ·06) and so uncertainties in it are unlikely to introduce significant errors into daily solar heating profiles. It does not seem necessary to take account of variation in surface waves, seawater turbidity and the angle of incidence of $I'(0)$ as a factor in albedo for models of oceanic solar heating.

The third group, oceanic absorption and scattering, is the most difficult to include in a model of the solar heating profile and there has been a tendency amongst climate modellers to simplify the problem rather drastically. Some authors (e.g. Bryan and Lewis 1979) have chosen to distribute $\dot{T}$ evenly over the top (depth H) ocean layer of their model:

$$\text{(A)} \qquad \dot{T}(z) = (1/Hc)I(0) \quad \text{for } 0 \leq z \leq H$$
$$= 0 \quad \text{for } z > H. \qquad (2)$$

Others (e.g. Kraus and Turner 1967) have distributed the daily temperature rise exponentially with depth:

(B) $$\dot{T}(z) = (1/c)I(0)\exp(-z/z_0). \quad (3)$$

We shall show later that such simplified parametrizations are inconsistent with observed vertical distributions of $I(z)$. Their adoption implies that the authors nevertheless believed them to be adequate for the purpose of modelling water mass conversion (A) and the structure of the seasonal thermocline (B). The first point, water mass conversion, has been discussed by Woods (1983, 1984) in the context of the thermal response of the ocean to CO_2 pollution of the atmosphere. He concluded that the problem demands a rather careful treatment of the oceanic boundary layer, including the solar heating profile. Simpson and Dickey (1981) have investigated the sensitivity of the upper ocean temperature profile and mixed layer depth to how the solar heating profile is parametrized. They concluded that method (B) leads to significant errors. The choice of a parametrization suitable for a global climatology of solar heating that will serve both purposes will be discussed in more detail later.

Whatever formulation is chosen, the vertical distribution will always depend on variables, such as z_0 in (B), whose values must be chosen to take account of the turbidity of the seawater. Jerlov (1976) introduced a widely used classification of seawater turbidity, based on measurements made in a wide variety of conditions. Charlock (1982) has shown that the annual cycle of the upper ocean temperature profile is sensitive to the water turbidity. An uncertainty as to whether the water should be classified as J(I) or J(II) can lead to an uncertainty in the surface temperature of greater than 1 K. That is more than the extra-tropical interannual variability (Barnett and Davis 1975; Weare 1977), so uncertainty in water turbidity could make the models useless for climate prediction based on such sea surface temperature anomalies. Jerlov (1976) has published a map giving a broad indication of the global distribution of seawater turbidity. It reflects the higher plankton concentrations in regions of plentiful nutrient supply (on the continental shelf, and at open ocean sites of upwelling and deep convection). But plankton concentration is patchy (Steele 1978) and exhibits large temporal variation, including a spring bloom in mid latitudes (Raymont 1980). There have been attempts to map the large-scale distribution of plankton (reviewed by Raymont) and to relate it to large-scale features of the ocean circulation (Reid 1977). Some progress has been made in developing computer models of the temporal variability of plankton concentration (Platt *et al.* 1977) and of their vertical distribution (Woods and Onken 1982). But not enough is yet known about the variations of plankton concentration to permit accurate calculation of the global, seasonal variation of ocean turbidity. The most promising development is global monitoring by satellite ocean colour scanner (Robinson 1983). Algorithms are being developed for extraction of a continuous variable, the ocean colour index (Jerlov 1976; Højerslev 1980), which can be related to the simpler Jerlov water type classification. The calculation of $I(z)$ from colour index measurements will require the use of algorithms derived empirically from *in situ* measurements, or from models of particulate scattering in the ocean (e.g. Raschke 1975).

To summarize, there seems to be a reasonable chance that within a decade we should have available global climatologies of the key variables controlling solar heating, namely: (1) The net downward flux of solar energy at the top of the ocean $I(0)$, from satellite observations or atmospheric general circulation models; and (2) the turbidity of the seawater, from satellite ocean colour scanner. Those projects will be major undertakings, involving programmes of *in situ* observations to support algorithm devel-

opment and calibration (Gienapp 1982). The results will not come quickly. Meanwhile, it is worth seeing how far one can proceed towards the target of a solar heating climatology on the basis of simple assumptions and existing data. That is the aim of the present study.

3. Aims and strategy of this study

This study is concerned mainly with the diurnal, seasonal and meridional variations of solar heating *below* the ocean mixed layer. It is well known from the literature (e.g. Charlock 1982) that the absorption of solar energy makes the temperature of water in the sub-polar seasonal thermocline rise each day until it becomes entrained into the mixed layer during autumn and winter. The daily temperature rise decreases with depth and becomes negligible below some limiting depth S. One of the questions to be answered by a climatology of solar heating is: "How deep must one go to be sure that solar heating is negligible for a particular purpose?". To answer the question it is necessary to establish a criterion for determining the value of S. We have considered two problems of climatological interest: ocean circulation dynamics, and the ocean heat budget.

In calculations of ocean circulation dynamics based on potential vorticity conservation (e.g. Olbers *et al.* 1982; Luyten *et al.* 1983) it is necessary to correct for changes in the spacing between isopycnals due to two diabatic processes: solar heating and turbulent diffusion (Schott and Zantop 1980). Inside the seasonal thermocline we expect the former to dominate; in the deep ocean the latter. That leads to the following criterion for S:

$$\text{at} \quad z = S, \qquad d_z\dot{T} = d_z^2(KT_z), \tag{4a}$$

where K is the diapycnic turbulent diffusivity, and $\dot{T}$ refers to solar heating only, as defined in Eq. (1). We do not know the value of K (Garrett 1979), but Eq. (4a) requires a specification of S in terms of $d_z\dot{T}$. Noting that the irradiance at depth S is nearly monochromatic we can make the approximation

$$d_z\dot{T}(S) = -\dot{T}(S)/L \tag{4b}$$

where L is the attenuation length for the deepest penetrating wavelength ($L = 28$ m at 480 nm). It is therefore sufficient to calculate the meridional and seasonal variations of the depth at which the more easily understood variable $\dot{T}$ has a constant value.

Another problem for which the value of S would be useful is heat budget studies of the upper ocean. Below what depth, S, is the accumulation of heat less than some specified value in a given interval of time? For the CO_2 response problem referred to in the introduction a suitable criterion for S is the depth below which the annual accumulation of energy is 10 MJ/m^{2}y. A daily energy accumulation criterion for S can be used to investigate the impact of the solar heating profile on seasonal and meridional response to slow thermal forcing of the ocean.

We are mainly concerned with solar heating *below* the mixed layer, in water that is stably stratified. The depth H of the mixed layer exhibits large diurnal and seasonal variations and responds rapidly to changes in the weather. On a calm sunny day it is not uncommon for the mixed layer to disappear completely, making it necessary to extend our study up to the surface. But over most of the globe (the night half, and much of the day half) there is a mixed layer whose depth has the same order of magnitude as S. The climatology of the mixed layer depth is complicated (Woods 1983) and not the subject

of this study; although, as we mentioned earlier, solar heating is an important factor in determining the value of H. Our strategy has been to take account of mixed layer depth variation in two ways. Firstly, the data are presented in terms of daily temperature rise in the mixed layer due to solar heating; recognizing, of course, that heat loss to the atmosphere is at the same time making the mixed layer temperature decrease. Secondly, the solar heating information will be presented at all depths up to the surface, regardless of the presence of a mixed layer. The reader should truncate the curves at the value of H that he believes to be appropriate for the particular location, date, time and weather of interest. Heat is not being lost to the atmosphere from below the mixed layer, so at depths greater than H the values indicate the actual temperature change of the water.

The requirements for solar heating information depend on the change of mixed layer depth during the time interval of interest in a particular scientific problem. For example, the problem may demand values of the instantaneous rate of solar heating quite close to the surface during the hours of daylight, when the mixed layer is shallow; or the daily totals of solar heating below the diurnal maximum depth of the mixed layer H_d, or the annual heating below the annual maximum depth of the mixed layer H_y. In order to meet these different needs we present the results in terms of hourly (T_h), daily (T_d), monthly (T_m) and annual (T_y) totals defined as follows:

$$T_t = \int_0^t \dot{T}\, dt'. \tag{5}$$

The diurnal, seasonal and meridional variations of solar heating are largely determined by the astronomical cycles of noon solar elevation and day length. Those changes are included in our calculations. Variation in the atmosphere (clouds, dust, etc) and in the ocean (plankton, sediment, etc) are also important but we make no attempt to take account of their regional and temporal variation, because we believe the available data might give misleading results. What we have done is to repeat the calculations (based on astronomical variation only) with different values of the cloud cover and seawater turbidity, as constant parameters. That leaves the reader to construct a climatology by selecting his own values for cloud cover and turbidity. It is worth noting, however, that the results for clear sky (no cloud) and clear seawater (no plankton) represent a limit that may be approached on sunny days in mid-ocean, where productivity is low. One can be confident that no solar heating (greater than the threshold value used in its definition) occurs deeper than S when it is calculated according to these limiting conditions.

4. Method

The calculations are based on the model described by Woods (1980), with the following modifications. Clouds were treated by a single variable, C, the total cloud cover. Seawater turbidity is expressed in terms of Jerlov's water types (Fig. 2). The parametrization of clouds and turbidity will now be discussed.

(*a*) *Clouds*

The following linear parametrization (based on Reed 1977; see also Simpson and Paulson 1979) was used to vary surface irradiance with cloud cover:

$$I'(0, C) = I'(0, 0)(1 - 0{\cdot}62C), \qquad \text{where } C \text{ varies from 0 to 1.} \tag{6}$$

In the Woods model the angle of incidence of solar radiation was not altered by the presence of clouds. Preliminary investigations showed that the results to be presented

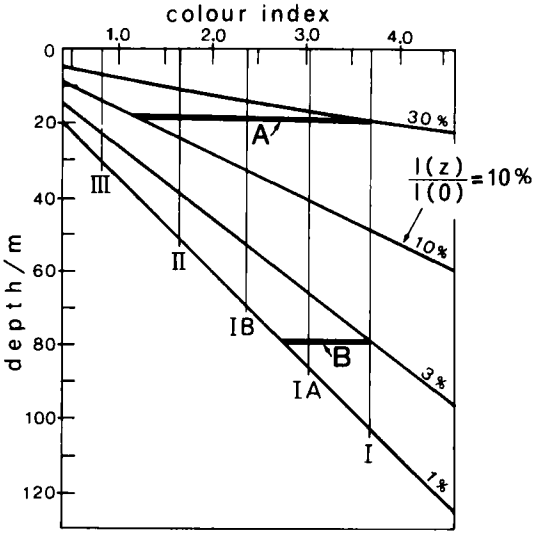

Figure 2. The Jerlov water type classification (labelled I, IA, IB, II and III) compared with the colour index used in satellite measurements of seawater turbidity (based on Højerslev 1980). The sloping lines are contours of constant ratio between the downward irradiance $I(z)$ and the surface irradiance $I(0)$. The two horizontal bars represent a change from clear to overcast sky. Bar A, at a depth of 15 metres, covers almost the whole range of seawater turbidity; bar B, at 80 metres, covers little more than one Jerlov type. It is concluded that at greater depths the uncertainty in seawater turbidity is more important than uncertainty in cloud cover.

later are not sensitive to the neglect of changes in variation of the zenith height distribution of $I'(0)$ with cloud cover. The error due to neglecting the change of angle of incidence of diffuse cloud radiation is likely to be masked by much larger uncertainty in the value of C, and the adoption of a simple linear relationship between $I'(0)$ and C. So we continued to follow the method of Woods (1980) in this study.

(*b*) *Seawater turbidity*

We defined type 0 water as the parametrization introduced by Woods (1980) in which the solar spectrum is divided into 27 spectral bands, each of which is absorbed according to Beer's law using coefficients for pure water. For more turbid water we used an empirical parametrization fitted to measurements made at the surface, and at a number of depths starting at one metre (Paulson and Simpson 1977). Following the approach of Simpson and Dickey (1981) we compared a number of parametrizations proposed in the literature (Table 1). The comparison led us to introduce the following new version for our study:

$$I(z) = I(0) \sum_{i=1}^{3} A_i \exp(-z/\lambda_i \cos \theta_s), \tag{7}$$

where θ_s is the zenith angle after refraction. The advantage of this three-exponential fit over the two-exponential fit suggested by Paulson and Simpson is shown in Table 2. Both parametrizations are constrained to pass through the measured value of $I(0)$, and are then fitted by the method of least squares to the subsurface observations. Despite the strong, unmeasured curvature in the top metre of the $I(z)$ profile, the three-exponential fit lies within 5% of the measured values at all depths. (The only exception is

TABLE 1. ALTERNATIVE PARAMETRIZATIONS OF DOWNWARD IRRADIANCE IN THE OCEAN

Depth variation	Comments
1. $I(0)(1 - z/H)$ (Bryan and Lewis 1979)	Ocean circulation models. H is the thickness of the first layer in the model.
2. $I(0)\exp(-z/\lambda)$ (Kraus and Turner 1967)	Early mixed layer models. λ is typically 30 m. Criticized by Simpson and Dickey (1981).
3. $I(0)\{A\exp(-z/\lambda_1) + (1 - A)\exp(-z/\lambda_2)\}$ (Paulson and Simpson 1977)	Widely used in mixed layer models. A, λ_1, λ_2 determined by fitting to measured values of $I(z)$.
4. $I(0)\exp(-z/\lambda_1)\{1 - A\tan^{-1}(-z/\lambda_2)\}$ (Zaneveld and Spinrad 1981)	Alternative to method 3.
5. $I(0)\sum_{i=1}^{27} A_i \exp(-z/\lambda_i \cos\theta_s)$ (Woods 1980, 1983c)	Spectral synthesis method based on pure water properties. Designed for studying diurnal variation of mixed layer depth in calm weather.
6. $I(0)\sum_{i=1}^{9} A_i \exp(-z/\lambda_i)$ (Simpson and Dickey 1981)	Simpler version of method 5. Used in studies of the diurnal thermocline based on Mellor–Yamada turbulence closure.
7. $I(0)\sum_{i=1}^{3} A_i \exp(-z/\lambda_i \cos\theta_s)$ (Horch, Barkmann and Woods 1983)	Parametrization used in this study. A_i and λ_i determined by fitting to the same measurements as 3 and 4. (See comparison in Table 2.)

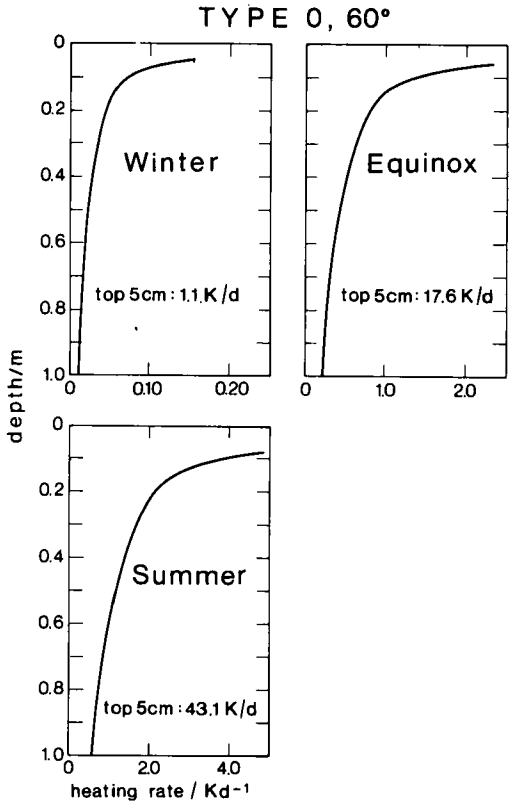

Figure 3a. The daily temperature rise in the top metre of the ocean for clear seawater (type 0) at latitude 60°. It is assumed that vertical mixing is complete in the top 5 cm but negligible below.

TABLE 2. COMPARISON OF ERRORS (%) IN DIFFERENT PARAMETRIZATIONS OF $I(z)/I(0)$

Depth z/m	Measured $I(z)/I(0)$ (Jerlov)	Spectral synthesis (5)*	Empirical (fit to data) (7)*	(3)*	(4)*	(2)**
	Type I	Type 0	Type I	Type I	Type I	Type I
		%	%	%	%	%
0	1	0	0	0	0	−52·7
1	0·445	6·3	−1·3	35·7	0	1·8
2	0·385	4·8	1·6	10·6	0·3	12·4
5	0·302	1·1	−0·3	−7·9	5·0	25·3
10	0·222	1·4	3·6	0·9	12·1	36·5
25	0·132+	−6·1	−0·8	−0·8	−3·9	16·7
50	0·053+	8·7	0·4	1·9	−20·7	−5·7
75	0·0168		(29·2)	31·0	−16·9	−1·8
100	0·0053		(66·0)	69·8	−12·3	1·9
150	0·00056		(162·5)	169·6	−8·2	1·8
200	0·000062				−8·1	−1·6
	Type II		Type II	Type II	Type II	
			%	%	%	
0	1		0	0	0	
1	0·420		−3·9	45·1	0	
2	0·347		1·5	16·0	−15	
5	0·234		3·2	−19·5	−19·9	
10	0·142		−1·0	−20·0	−15·3	
25	0·042		−2·6	−8·2	−3·9	
50	0·0070		2·5	−7·6	1·9	
75	0·00124		4·6	−12·6	3·2	
100	0·000228		3·0	−20·3	1·3	
150	0·0000080		3·9	−36·1	6·0	

* Method, as listed in Table 1.
** Fitted to the four deepest measured values of $I(z)/I(0)$.
( ) Values calculated by method 2 were used to obtain type I results in the present study.
+ Measured values for type I are suspect at these depths.

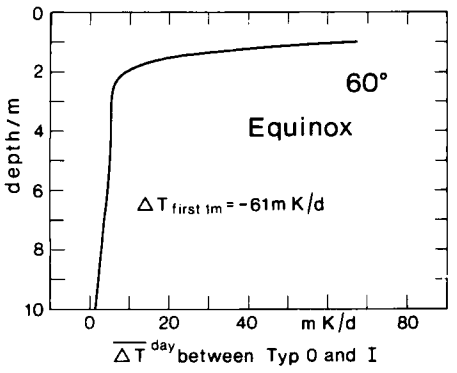

Figure 3b. Difference between daily temperature rise between types 0 and I in the top 10 metres.

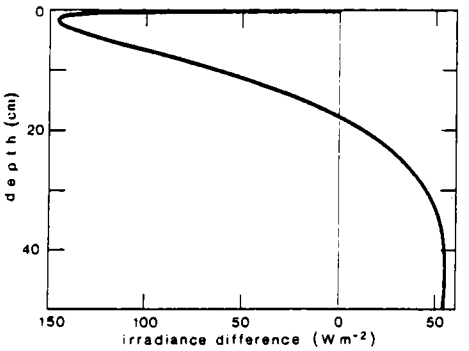

Figure 3c. The difference between the downward irradiance profiles in the top 50 cm of the ocean calculated for water type 0 (parametrized by the 27 spectral band synthesis) and type I (using the three exponential empirical fit to measurements below one metre).

at depths greater than 50 m for type I water, where, as Paulson and Simpson have already noted, Jerlov's data contain internal inconsistencies; see Horch *et al.* (1983) and Table 2 for more details.) On the other hand, the two-exponential fit involves errors of up to 40% in the top 10 m. Errors of that magnitude can be important in climate problems such as the thermal response of the ocean to atmospheric CO_2 pollution.

It should not be forgotten that approximately half of the total solar heating of the ocean occurs in the top one metre (Ivanoff 1977). Not having measurements of the $I(z)$ profile in the top metre, we prefer to model it by the Woods (1980) spectral synthesis involving 27 pure water absorption coefficients (Fig. 3(a)). Table 2 shows that this synthesis method gives values that deviate by less than 9% from the Jerlov measurements characterizing type I water, in the top 50 m. Our justification is that even in moderately turbid water (Jerlov type IA or IB, say) the scatterers need a thicker layer of water significantly to alter $I(z)$. In fact the difference between the daily solar heating profile $T_d(z)$ calculated by the type 0 synthesis and the type I empirical parametrization is less than 5 mK/d in the depth range 3 to 10 m (Fig. 3(b)). The difference in the irradiance profile in the top half metre is shown in Fig. 3(c).

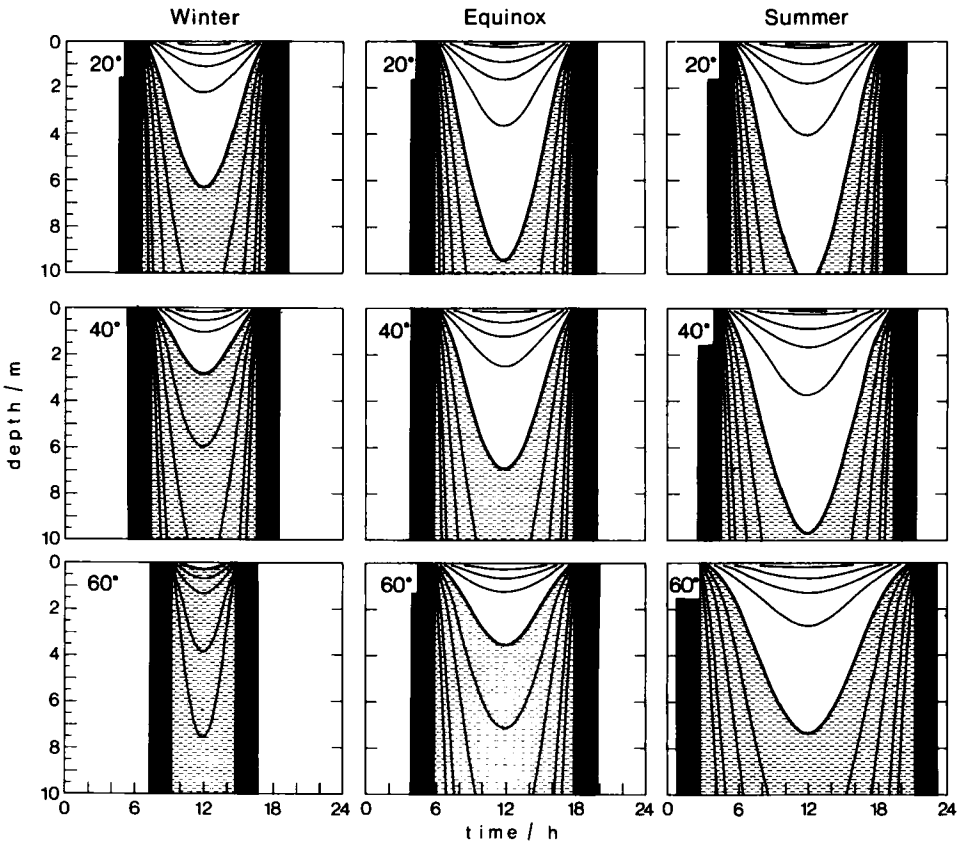

Figure 4a. Diurnal variation, at the latitudes shown, of the rate of temperature rise due to solar heating in the top 10 metres (type 0). Contours of constant T_h are given at the following values: 0·5, 1, 2·5, 5, 10, 25, 50, 100, 250 & 500 mK/h. The shading starts at 10 mK/h.

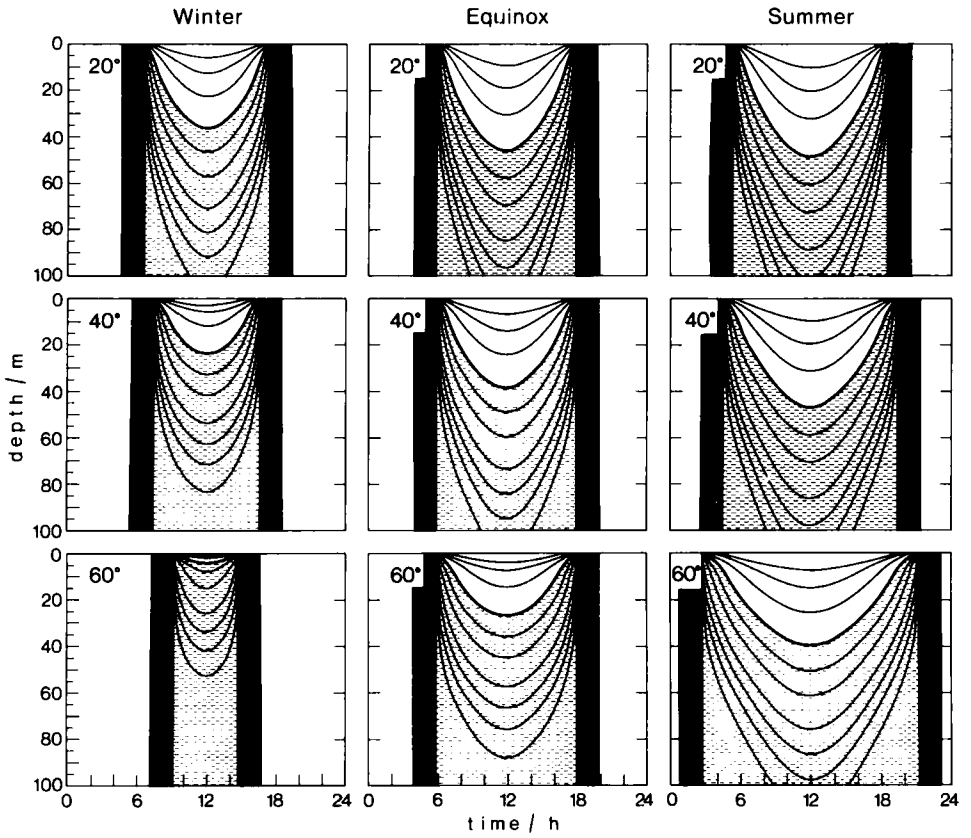

Figure 4b. Diurnal variation of the rate of temperature rise due to solar heating in the top 100 metres (type IB). Contours of constant T_h are given at the following values: 0·01, 0·025, 0·05, 0·1, 0·25, 0·5, 1, 2·5, 5 and 10 mK/h. The shading starts at 1 mK/h.

5. Results

Here we present a selection of products from the solar heating model used in this study. The aim is to illustrate the most important features of the climatology of solar heating, including the diurnal, seasonal and meridional variation of heating at different depths, and their sensitivity to cloud cover and seawater turbidity. A much larger selection of products, and details of the computer model used to generate them is available in a report of the Institut für Meereskunde (Horch *et al.* 1983).

The dominant variation in solar heating of the ocean, the diurnal cycle, is illustrated in Fig. 4. A detailed knowledge of the diurnal variation of solar heating is needed for studies of upper ocean convection (Woods 1980) and related phenomena, such as phytoplankton growth (e.g. Woods and Onken 1982). The heating in the top 10 m, shown in Fig. 4(a), is particularly relevant for such studies; it is based on the pure water parametrization (type 0) in order to overcome the difficulties arising when using the empirical parametrization in the top few metres close to the data cut-off at 1 m depth.

At greater depths it is possible to use the empirical parametrization. The diurnal variation of solar heating in the top 100 m is shown in Fig. 4(b), in which Jerlov water type IB has been chosen as typical of the open ocean. The increasing importance of seasonal variation of day length as one goes to higher latitude is clearly seen in Fig. 4.

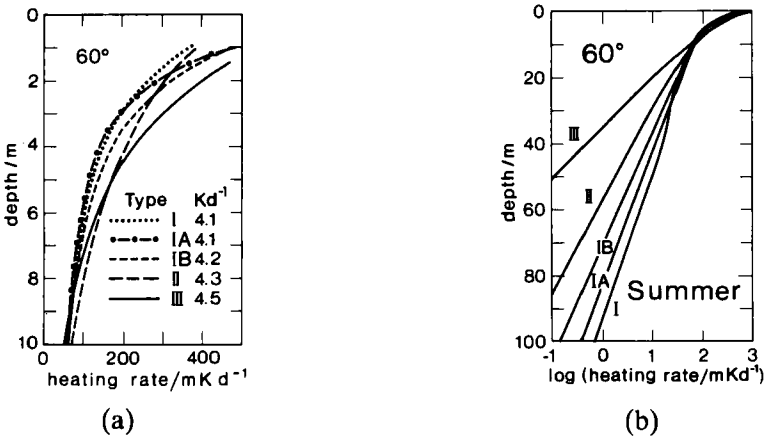

Figure 5. The effect of seawater turbidity on the daily rise in temperature due to solar heating below the mixed layer. (a) The top 10 metres. (b) The top 100 metres.

The diurnal variation on the equator at the equinoxes is similar to that at 20° latitude at the summer solstice; the equatorial solstices are like the 20° equinox.

From now on the results will refer to the daily total heating T_d and the daily total energy flux I_d. Figure 5 is concerned with the effect of seawater turbidity on the profile of daily temperature rise due to solar heating. Figure 5(a) shows the different forms taken by $T_d(z)$ calculated using the empirical parametrization for types I, IA, IB, II and III in the depth range 1 to 10 m. Despite some apparent eccentricities, the curves accurately reflect the measurements used in the three-exponential fit. The inset table shows the vertically averaged temperature rise in the top one metre for each water type. In deeper water (Fig. 5(b)) the effect of changing turbidity becomes more systematic.

Even in calm weather convection deepens at night mixing the water warmed during the previous day; and in windy weather mixing persists throughout the day, albeit with a noticeable diurnal variation of mixed layer depth. When we consider the daily heat input, what matters is the maximum depth H_d that the mixed layer reaches in the 24-hour period. The daily temperature rise in the mixed layer due to solar heating, taken in isolation from other processes (i.e. cooling to the atmosphere and advective flux divergence), is shown in Fig. 6. It is seen that the curve is rather insensitive to seawater

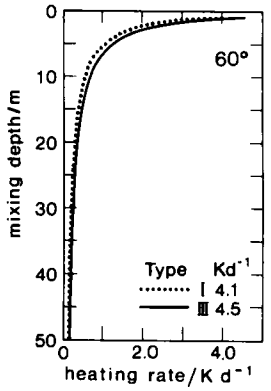

Figure 6. The daily rise in temperature of the mixed layer at 60° latitude on the summer solstice, as a function of the maximum depth of the mixed layer during the day. The tabulated values give the temperature rise in the top metre for types I and III. N.B. The actual temperature rise will be lower because of heat loss from the mixed layer to the atmosphere.

turbidity. That is because most of the solar heating occurs close to the surface. Changes in turbidity only influence the curve through their effect on the penetration of solar energy to depths greater than H_d. This plot provides the best justification for treating solar heating by method (A) in ocean models (see Eq. 2). But there are some climate problems for which that parametrization is inadequate, and it becomes important to know how much heat is absorbed below the mixed layer.

The meridional and seasonal variation of solar heating below the mixed layer is illustrated in Figs. 7 to 12. The first two address the problem of the maximum depth of solar heating. We noted earlier that for some problems it is useful to specify the limiting depth S in terms of the rate of temperature change. Figure 7 shows the depth distribution of S defined by $T_d = 1$ and 10 mK/d for two typical seawater turbidities IA and II. For

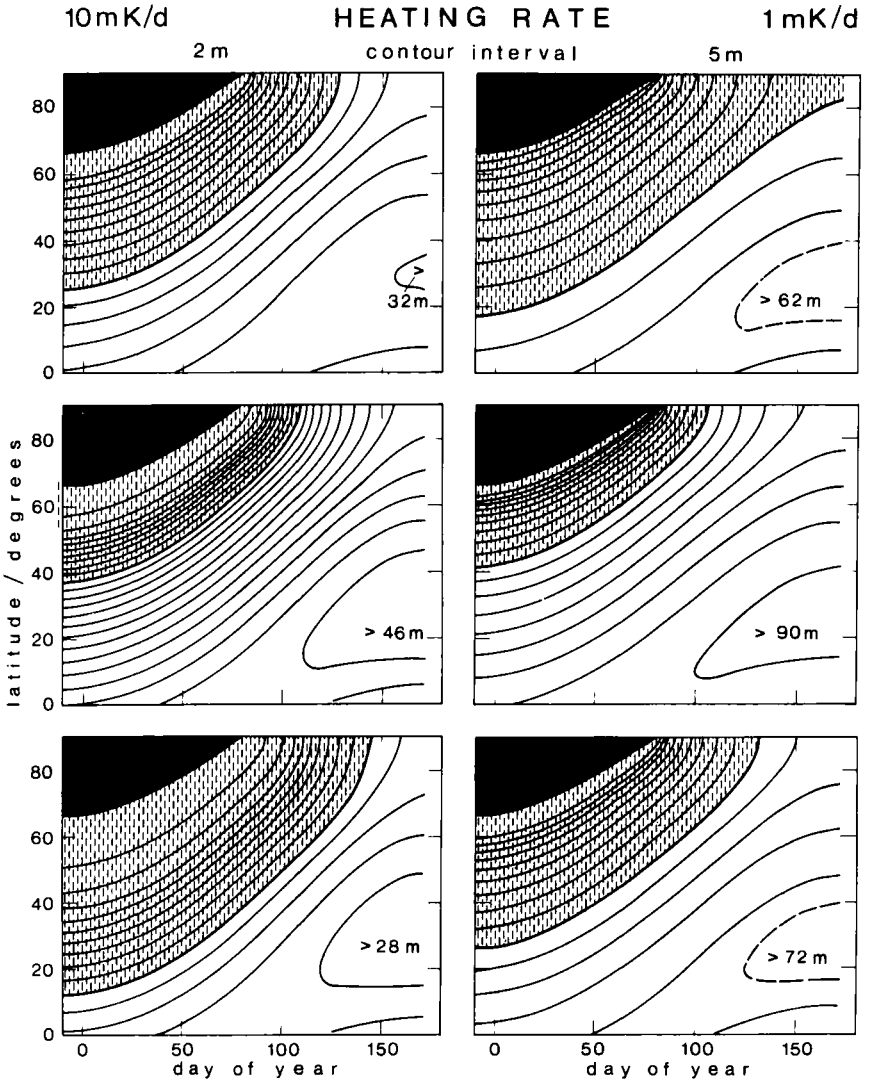

Figure 7. The seasonal and meridional variation of the depth of the surface at which the daily increase in temperature is 1 and 10 mK/d. Shading starts at 20m (left) and 50m (right).

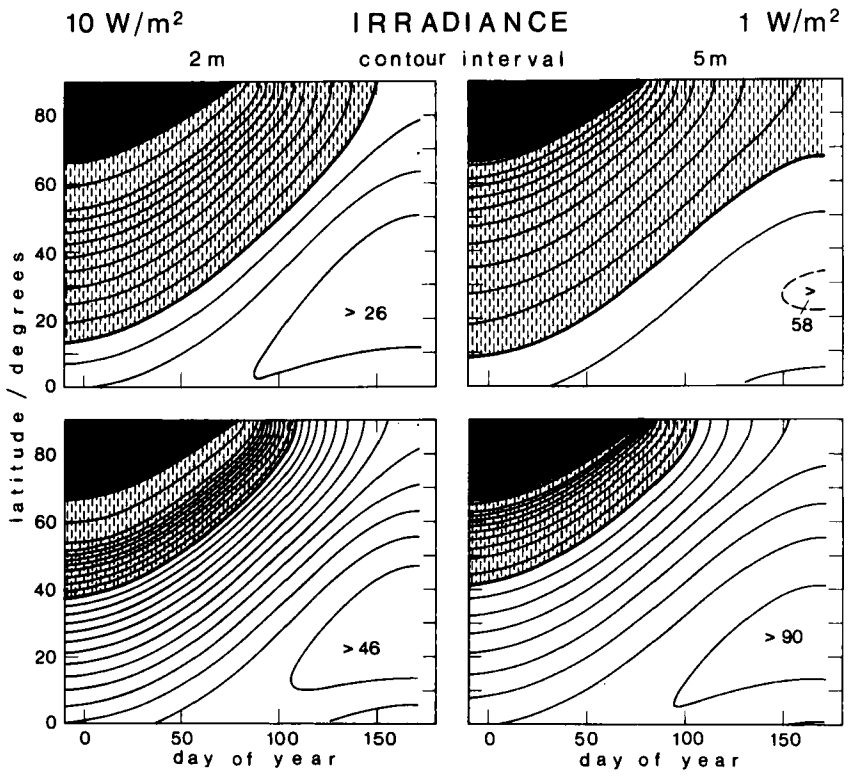

Figure 8. The seasonal and meridional variation of the depth of the surface at which the daily mean downward irradiance is 1 and 10 W/m². Shading starts at 20m (left) and 50m (right).

other purposes it is more useful to define S in terms of the energy flux. Figure 8 shows the depth distribution of S defined by $I_d = 86.4$ and 864 KJ/m²d for the same two turbidities (1 W/m² = 86·4 KJ/m²d). The upper four panels of Fig. 7 have been based on clear skies ($C = 0$), so they represent the limiting case. The lower two panels show the effect of increasing cloud cover to 100% when the seawater has type IA turbidity. It is concluded that the daily accumulation of solar energy below the mixed layer, and therefore the depth S, is as sensitive to changes of seawater turbidity as of cloud cover.

The seasonal and meridional variations of daily temperature rise and daily energy flux at constant depths are shown in Figs. 9 and 10. Here we explore more thoroughly the influence of seawater turbidity, covering the full range of Jerlov water types. The depths chosen lie below the mixed layer in most of the tropics and at higher latitude in summer. The calculations have been made for a clear sky; correction for cloud cover can be made using the linear formula given in Eq. (6). As in Figs. 7 and 8, we note the large seasonal variation in the meridional variation of solar heating. The location of the maximum, which reaches the tropics at the summer solstice, reflects the relative importance of noon zenith angle compared with day length at low latitudes.

This section on seasonal and meridional variation is completed with two illustrations of the vertical distribution of the daily temperature rise. Figure 11 shows the seasonal variation of $T_d(z)$ at three latitudes, and Fig. 12 shows the meridional variation of $T_d(z)$ at the solstices and equinoxes. In both cases the calculations are for two water types

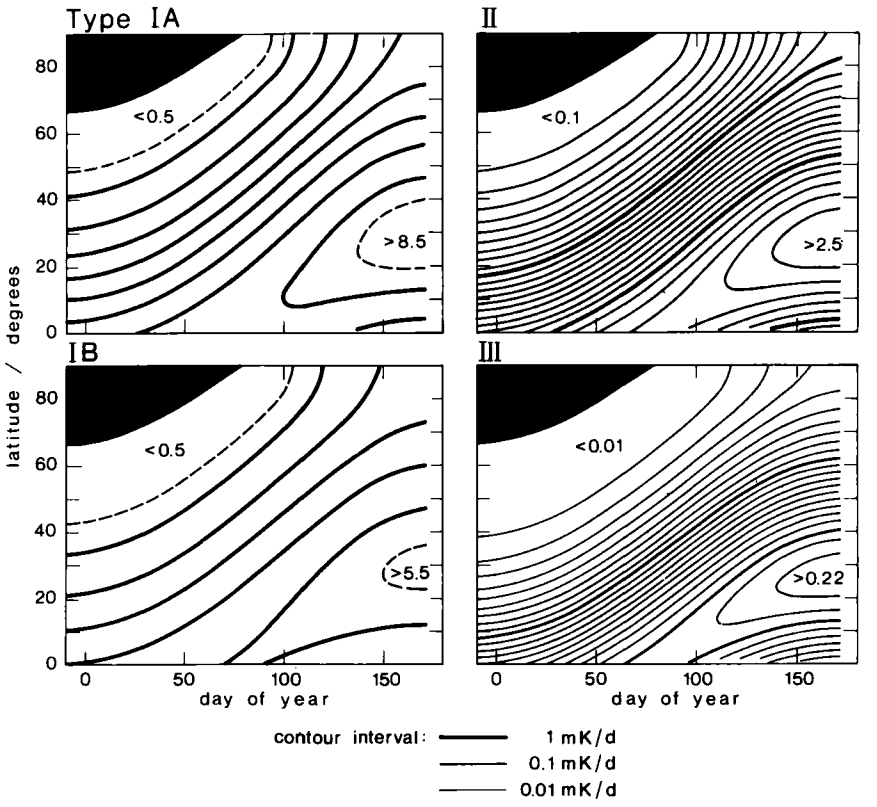

Figure 9. The seasonal and meridional variation of the daily rise in temperature at a depth of 50 metres, for Jerlov types IA, IB, II and III.

(IA and III) and for a cloud-free sky. The reader can easily adjust the values of $T_d(z)$ for different cloud cover using Eq. (6).

Next we consider the annual cumulative temperature rise at a fixed depth below the mixed layer (Fig. 13) and the cumulative heat storage below that depth (Fig. 14). Remember that the temperature rise shown in Fig. 13 does not include processes other than solar heating. The S curves in Fig. 16 were derived from annual integrations similar to those shown in Fig. 14 repeated at latitude intervals of 5°.

It is also important to remember that the temperature change plotted in Fig. 13 and the heat storage plotted in Fig. 14 are due solely to local solar heating. In most places, advection also makes an important contribution to the observed temperature change. The relative contributions of advection and solar heating below the mixed layer at OWS 'C' (35°W 52°30'N) are compared in Fig. 15, where the solar heating has been calculated using the observed monthly mean cloud cover (Bunker and Goldsmith 1979) and seawater type IB. The advection of heat into the North Atlantic Ocean supplies the difference between the annual cooling to the atmosphere and the total annual solar heating.

6. Discussion

One of the motivations for this investigation was the problem of calculating the thermal response of the ocean to the changing IR flux at the surface induced by

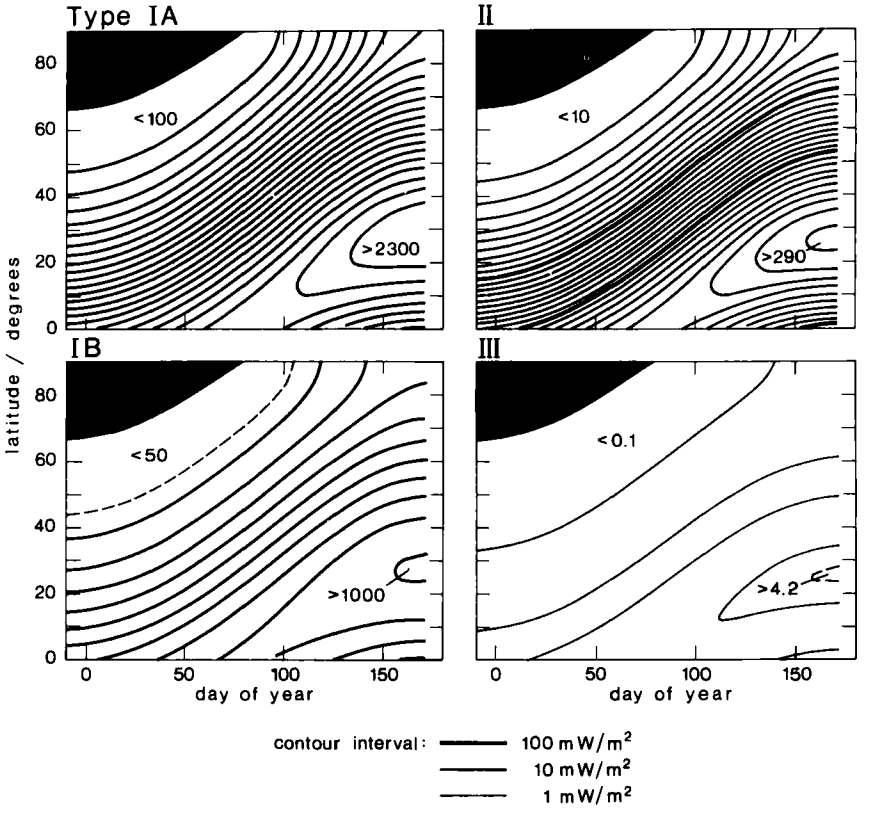

Figure 10. The seasonal and meridional variation of the daily accumulation of heat below a depth of 75 metres, for Jerlov types IA, IB, II and III. (1 W/m^2 = 86.4 KJ/m^2 d)

atmospheric CO_2 pollution. As pCO_2 rises, the net IR cooling of the ocean decreases by an amount that can be calculated from atmospheric radiation transfer theory (Ramanathan 1981). Heat (from absorption of solar radiation) accumulates in the ocean until the surface temperature has risen sufficiently for enhanced evaporation, conduction and thermal radiation to restore the global annual heat balance. There is a lag between the greenhouse forcing and the surface temperature response. Calculation of the lag is one of the key elements in any prediction of climate response to CO_2 pollution. Early calculations, based on the assumption that the heat anomaly occurs only in the ocean mixed layer, gave unrealistically short lag times. More recent predictions, which include Ekman pumping of the heat anomaly into the warm water sphere, suggest a lag of a few decades (Bryan *et al.* 1982). When the lag becomes so long, it is necessary to take account of the displacement of the anomaly by ocean currents. The redistribution influences the regional and seasonal temperature change both during the transient response and in equilibrium. In order to simplify the analysis of the transient response, let us assume that the greenhouse forcing is uniform and that it does not change the solar heating, mixed layer depth and ocean currents. The transient response can then be predicted as though the CO_2-induced heat anomaly were a passive tracer introduced with the same source distribution (Bretherton 1982). The contribution of this paper to

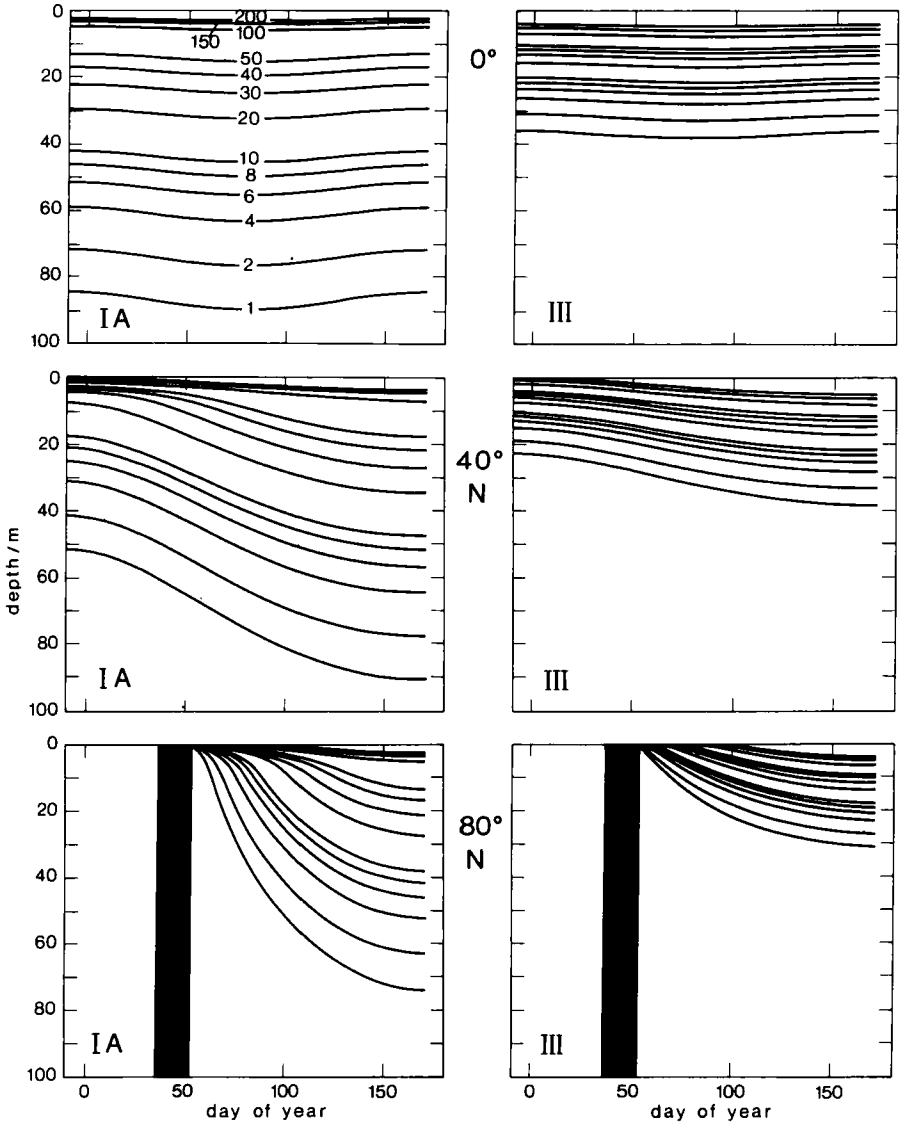

Figure 11. The seasonal variation, at latitudes 0°, 40°N and 80°N, of the depths at which the daily temperature rise due to solar heating has values in the range 1–200 mK/d, for Jerlov types IA and III.

the CO_2 response problem is to clarify the nature of the source (i.e. solar heating) distribution.

The key aspect of the solar heating source function is the partitioning between heating in and below the mixed layer. The former directly influences the surface temperature and contributes to the Ekman transport of heat. The latter does not influence surface temperature, except through its impact on mixed layer depth which is not being considered at this level of simplification, and the heat anomaly it produces is displaced by the geostrophic, but not by the Ekman flow. Let us start with the secular change (seasonal modulation will be discussed later). We can divide the world ocean into two regimes depending on the relative annual maximum depths of solar heating (S) and of

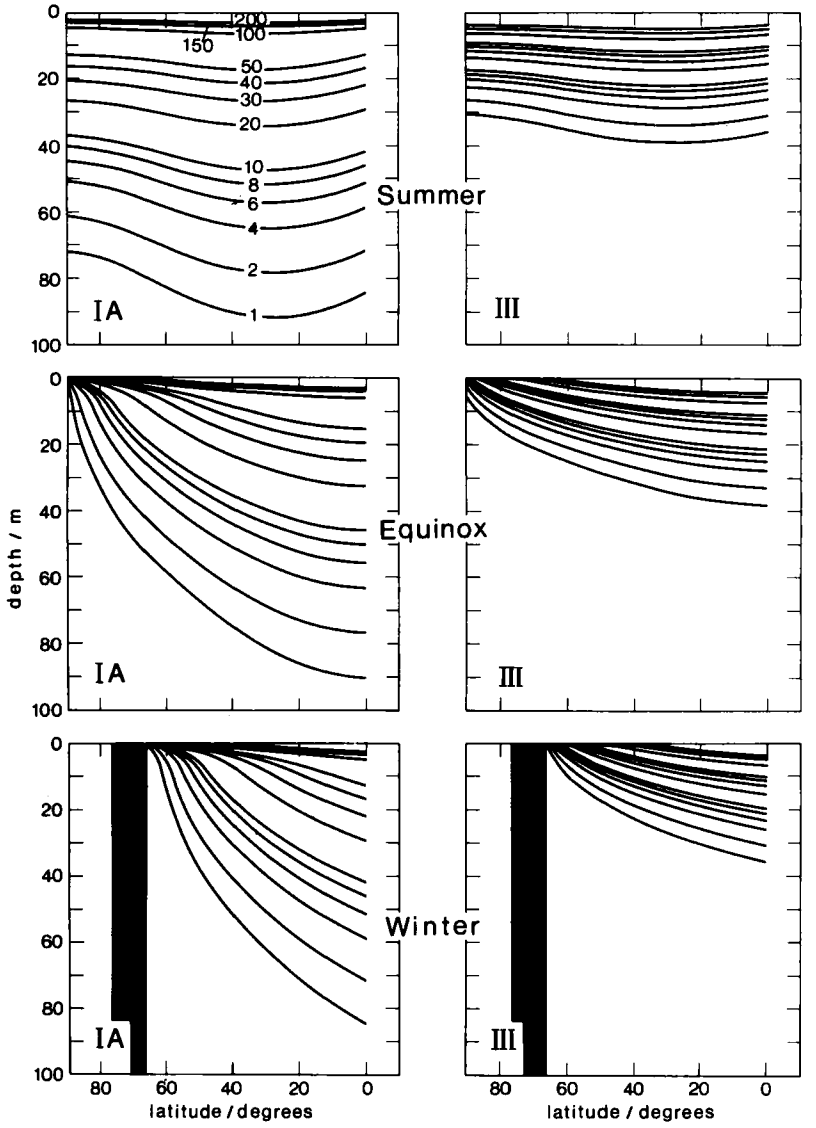

Figure 12. The meridional variation, at the solstices and equinox, of the depths at which the daily temperature rise due to solar heating has values in the range 1–200 mK/d, for Jerlov types IA and III.

the mixed layer (H_{max}). Figure 16 shows the variations of S and H_{max} along 30°W in the North Atlantic. Significant solar heating occurs below the mixed layer at all seasons in the tropics, but only in the summer (H_{min}) at higher latitudes. The S curves were calculated by annual integrations of solar heating assuming no cloud and water type IA. The correction for cloud amount can easily be made using Eq. (6); the correction will be less than $\frac{1}{3}$ of the spacing between the S lines for 10 and 100 MJ/m^{2}y. The sensitivity to change of ocean turbidity is greater. Figure 14 shows that a change from type I to type IB alters the annual heat storage below the mixed layer by approximately ± 100 MJ/m^{2}y. That range of turbidity roughly represents the uncertainty in the present state of knowledge. So the uncertainty in the annual accumulation of heat below the

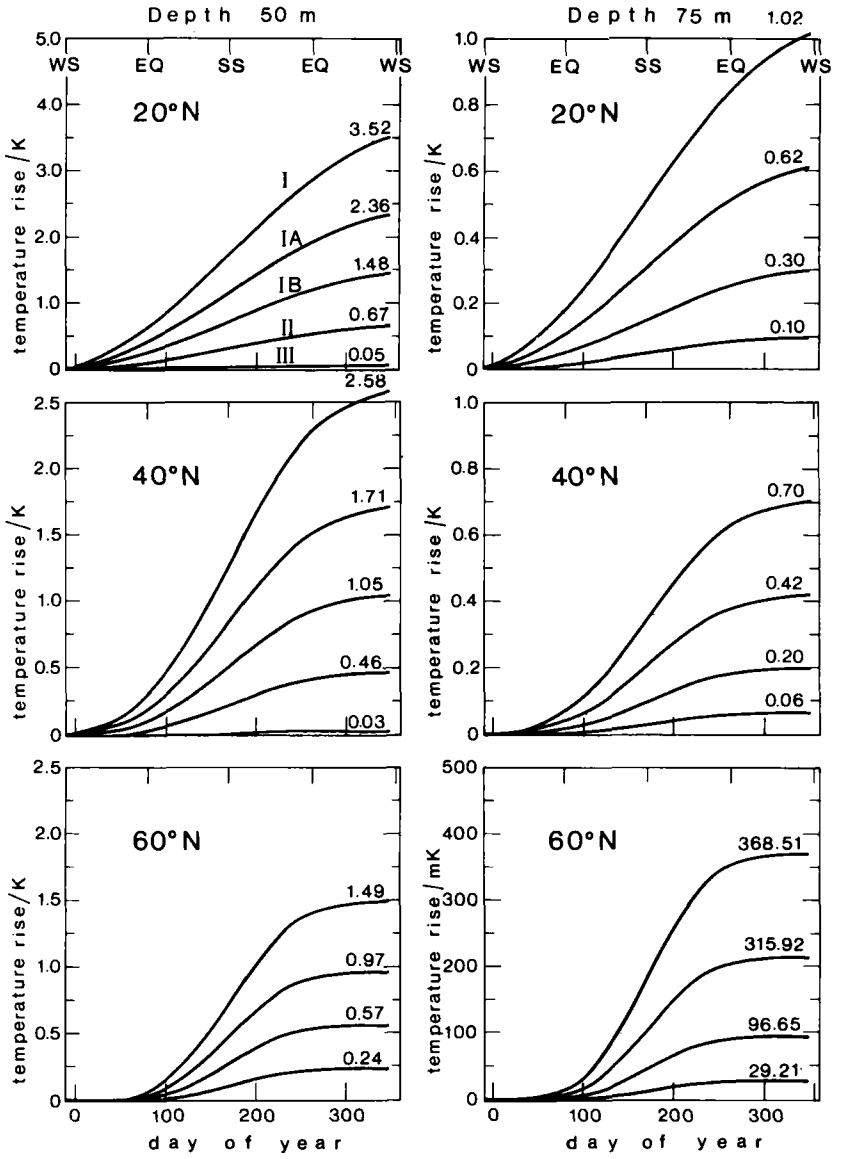

Figure 13. Progression through the year of temperature rise due to solar heating at constant depth for Jerlov types I, IA, IB, II and III. Values of T_y are indicated; values of T_m can be extracted from the curves.

tropical mixed layer is greater than the greenhouse effect on surface IR due to doubled pCO_2. This uncertainty is important in calculations of the transient thermal response of the ocean to CO_2 pollution, because the geostrophic flushing of heat from the tropics into the outer regime where H_{max} exceeds S is slow compared with the flushing by Ekman flow in the mixed layer. The geostrophic escape time from the tropical Pacific, which provides over half the area of the tropical oceans, is particularly long because of its breadth.

Ekman suction brings the sun-warmed water up into the mixed layer in less than half of the area of the tropics; elsewhere the water is pumped down. The annual

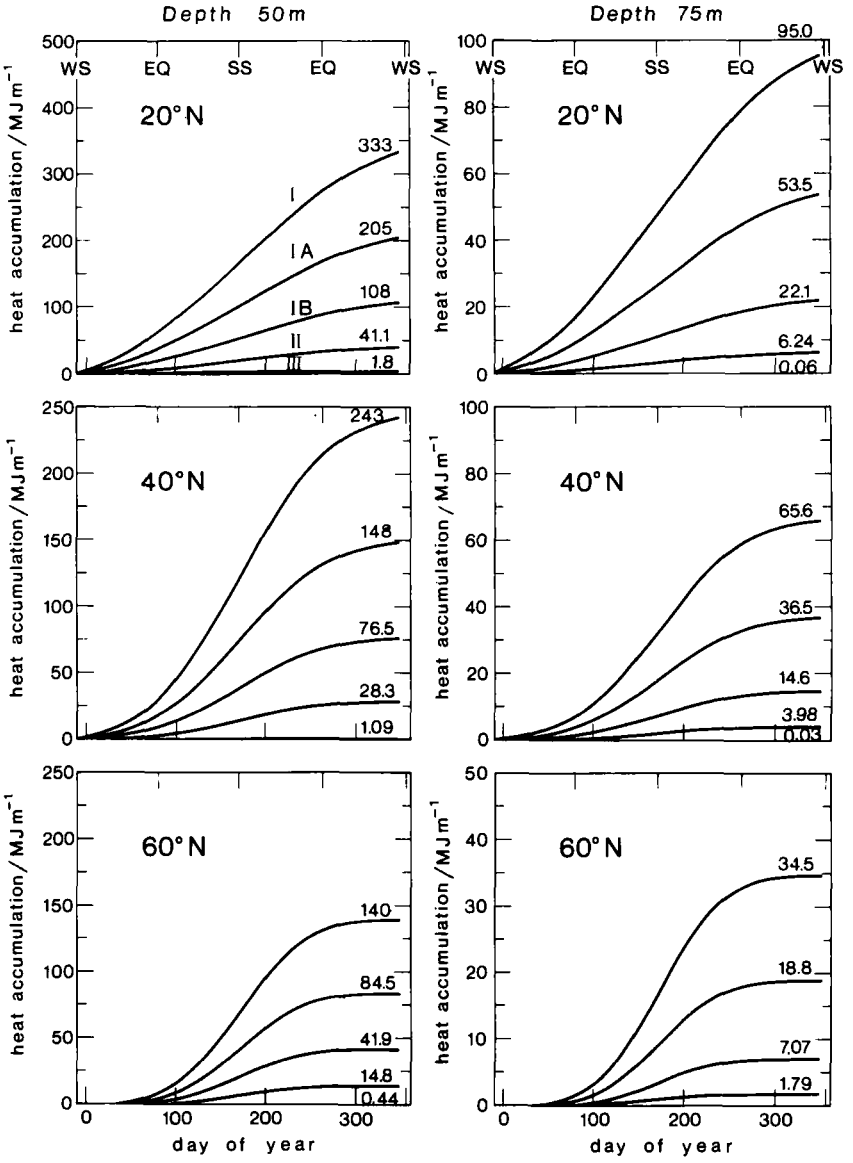

Figure 14. Heat accumulation during the year below a fixed depth at three latitudes, for Jerlov types I, IA, IB, II and III.

temperature rise of water that escapes entrainment into the mixed layer can exceed 1 K/y (Fig. 13). Such a rise will lead to deepening of the mixed layer. The nutrient supply to the euphotic zone will then rise, and lead to an increase in primary productivity. More phytoplankton mean greater seawater turbidity and lower CO_2 outgassing. Detailed modelling of those processes requires an ocean circulation model. The purpose of the present discussion is to point out that the tropical sub-mixed-layer heating rates calculated in this paper are so large that they may not safely be ignored in predictions of climate response to CO_2 pollution. Outside the tropics, solar heating occurs below the mixed layer only during the summer (see Fig. 16). Its neglect leads to a mixed layer temperature

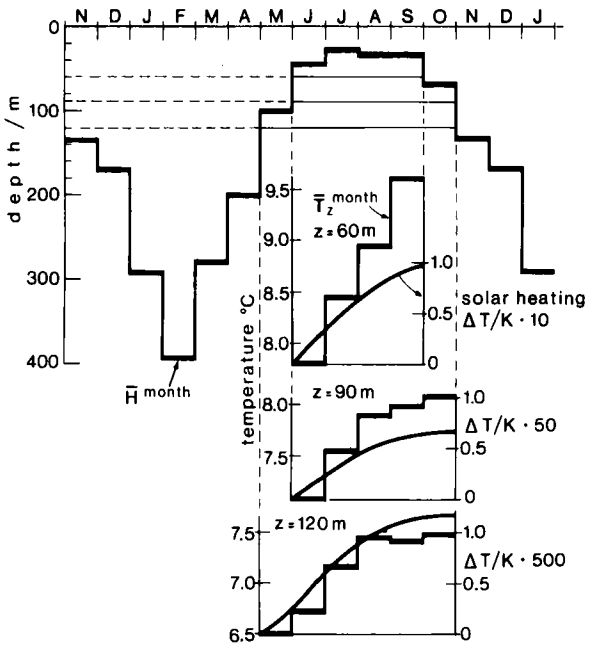

Figure 15. A comparison of the relative contributions of solar heating and advection to the observed temperature rise below the mixed layer at Ocean Weather Station "C".

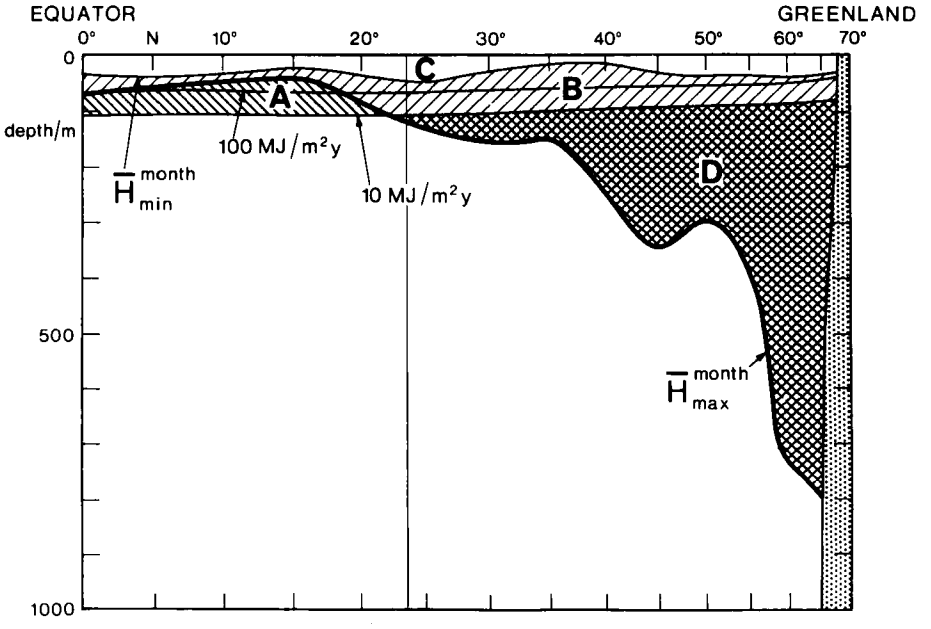

Figure 16. A section along 30°W in which the maximum depth of annual solar heating (for clear skies and type 1A water) is compared with the extrema of H, the monthly mean mixed layer depth (according to Robinson *et al.* 1979). Water warmed by the sun is never mixed in region A, is mixed during the winter in region B, and is mixed during all months of the year in region C. In region D, winter mixing extends below the maximum depth of solar heating. (Equal area projection.)

a few tenths of a degree too high in summer, but deep winter mixing dilutes the heat anomaly permitting only a small secular trend. Although an oceanic global circulation model will be needed to compute the full details of the transient response, the study of solar heating presented in the paper shows that there is potential for a far more rapid response in the tropics than at high latitudes.

7. Conclusion

It is important to know how the vertical distribution of solar heating in the ocean varies regionally and seasonally. It influences the depth of convection and therefore the rate of upward heat transport in the upper ocean. And a significant fraction of the solar energy entering the ocean is absorbed below the annual maximum depth of the mixed layer, and can therefore escape to the atmosphere only after lateral displacement by ocean currents. Rather accurate calculation of the vertical profile of solar heating is needed to meet the requirements of climate prediction, involving anomalies of sea surface temperature occurring naturally from year to year due to random forcing by the weather, or as a trend over several decades due to atmospheric pollution. The results of the present study are also relevant to the correction of diabatic effects in diagnostic studies of upper ocean circulation. They show that the rate of temperature rise in the mixed layer due to solar heating is controlled by the surface energy flux, $I'(0)$, which depends on the astronomical cycles and atmospheric variables, in particular the cloud cover. But the rate of solar heating below the mixed layer depends more on the turbidity of the seawater than on the cloud cover. At present there is considerable uncertainty in the regional and seasonal variations of both cloud cover and seawater turbidity. When those uncertainties have been removed by research now in progress (including the International Satellite Cloud Climatology Project, and the analysis of Coastal Zone Colour Scanner data) it will become possible to calculate a formal climatology of solar heating of the ocean. Meanwhile, the main features of such a climatology have been revealed by the present study.

References

Barnett, T. P. and Davis, R. E. 1975 'Eigenvector analysis and prediction of sea surface temperature fluctuations in the North Pacific Ocean', pp. 439–450 of Proc. Symp. Long term climatic fluctuations, WMO Technical Note No. 421

Bretherton, F. P. 1982 Ocean climate modelling. *Progr. Oceanogr.*, **11**, 93–129

Bryan, K., Komro, F. G., Manabe, S. and Spelman, M. J. 1982 Transient climate response to increasing atmospheric carbon dioxide. *Science*, **215** 56–58

Bryan, K. and Lewis, L. J. 1979 A water mass model of the World Ocean. *J. Geophysical Res.*, **34**, 2503–2517

Bunker, A. F. and Goldsmith, R. A. 1979 Archived time-series of Atlantic Ocean meteorological variables and surface fluxes. Technical report. WHOI-79-3, Woods Hole Oceanographic Institution

Charlock, T. P. 1982 Mid-latitude model analysis of solar radiation, the upper layers of the ocean, and seasonal climate. *J. Geophysical Res.*, **87**, 8923–8930

Garrett, C. 1979 Mixing in the ocean interior. *Dyn. Atmos. Ocean*, **3**, 239–266

Gautier, C. 1982a 'Daily shortwave energy budget over the ocean from geostationary satellite measurements', pp. 201–206 of *Oceanography from Space*, (Ed. J. F. R. Gower), Plenum, New York

1982b Satellite measurements of insolation over the Tropical Oceans. *Tropical Ocean–Atmosphere Newsletter*, **12**, 5–6

Gautier, C., Diak, G. and Masse S. 1980 A simple model to estimate incident solar radiation at the

surface from GOES satellite data. *J. Applied Met.*, **19**, 1005–1012

Gienapp, H. 1982 Optical properties of seawater in the German Bight and the mouth of the Elbe; the 1978 CZCS prelaunch experiment of the Deutsches Hydrographic Institut. *Deutsche Hydrographischen Z.*, **35**, 136–167

Hinzpeter, H. 1980 'Atmospheric radiation instruments', pp. 491–507 of *Air-Sea Interaction: Instruments and Methods*, (Ed. F. Dobson, L. Hasse and R. Davis), Plenum, New York

Højerslev, N. K. 1980 Water colour and its relation to primary production. *Boundary-Layer Met.*, **18**, 203–220

Horck, A., Barkmann, W. and Woods, J. D. 1983 *Die Erwärmung des Ozeans hervorgerufen durch solare Einstrahlung*. Kiel: Institut für Meereskunde, Bericht No 120

Ivanoff, A. 1977 'Oceanic absorption of solar energy', pp. 47–71 of *Modelling and prediction of the upper layers of the ocean* (Ed. E. B. Kraus). Pergamon, Oxford

Jerlov, N. G. 1976 *Marine optics*. Elsevier, Amsterdam

Kondratyev, K. Ya. 1969 *Radiation in the atmosphere*. Academic Press, New York

Kraus, E. B. and Turner, J. S. 1967 A one-dimensional model of the seasonal thermocline. II: The general theory and its consequences. *Tellus*, **19**, 98–106

Luyten, J. R., Pedlosky, J. and Stommel H. 1983 The ventilated thermocline. *J. Physical Oceanogr.*, **13**, 292–309

Olbers, D., Willebrand, J. and Wenzel M. 1982 The inference of ocean circulation from climatological hydrographic data. *Ocean Modelling Newsletter*, **46**, 5–9

Oort, A. H. and Vonder Haar, T. H. 1976 On the observed annual cycle in the ocean–atmosphere heat balance over the northern hemisphere. *J. Physical Oceanography*, **6**, 781–800

Paulson, C. A. 1980 'Oceanic radiation measurements', pp. 509–521 of *Air–Sea Interaction: Instruments and Methods*, (Ed. F. Dobson, L. Hasse and R. Davis), Plenum, New York and London.

Paulson, C. A. and Simpson, J. J. 1977 Irradiance measurements in the upper ocean. *J. Physical Oceanography*, **7**, 952–956

Paltridge, G. W. and Platt, C. M. R. 1976 *Radiative processes in meteorology and climatology*. Elsevier, Amsterdam

Payne, R. E. 1972 Albedo of the sea surface. *J. Atmos. Sci.*, **29**, 959–970

Platt, T., Denman, K. and Jassby A. D. 1977 'Modeling the productivity of phytoplankton', pp. 807–856 of *The Sea* **6**, (Ed. E. D. Goldberg, I. N. McCave, J. J. O'Brien and J. H. Steele).Wiley-Interscience, New York

Ramanathan, V. 1981 The role of ocean–atmosphere interaction in the CO_2 climate problem. *J. Atmos. Sci.*, **38**, 918–930.

Raschke, E. 1975 Numerical studies of solar heating of an ocean model. *Deep-Sea Res.*, **22**, 659–665

Raymont, J. E. G. 1980 *Plankton and productivity in the Sea. I: Phytoplankton*. Pergamon, Oxford

Reed, R. K. 1977 On estimating insolation over the ocean. *J. Phys. Oceanogr.*, **7**, 482–485

Reid, J. 1977 'Some thoughts on the dependence of sound speed and scattering layers upon circulation', pp. 15–64 of *Ocean sound scattering prediction*, (Ed. N. R. Anderson and B. J. Zahuranec), Plenum, New York & London

Robinson, I. S. 1983 Satellite observations of ocean colour. *Phil. Trans. Roy. Soc. London*, **A 309**, 415–432

Robinson, M. K., Bauer R. A. and Schroeder, E. H. 1979 *Atlas of North-Atlantic–Indian-Ocean monthly mean temperatures and mean salinities of the surface layer*. US Naval Oceanographic Office, Ref. Pub. 18

Schott, F. and Zantop, R. 1980 On the effect of vertical mixing on the determination of absolute currents by the beta spiral method. *Deep-Sea Res.*, **27**, 173–180

Simpson, J. J. and Dickey, T. D. 1981 Alternative parameterizations of downward irradiance and their dynamical significance. *J. Physical Oceanography*, **11**, 876–882

Simpson, J. J. and Paulson, C. A. 1979 Mid-ocean observations of atmospheric radiation. *Quart. J. Roy. Met. Soc.*, **105**, 487–502

Steele, J. H. (editor) 1978 *Spatial patterns in plankton communities*. Plenum, New York

Tyler, J. E. and Smith, R. C. 1970 *Measurements of spectral radiance underwater*. Gordon and Breach, New York

Weare, B. C. 1977 Empirical orthogonal analysis of Atlantic Ocean surface temperatures. *Quart. J. Roy. Met. Soc.*, **103**, 467–478

Woods, J. D. 1980 Diurnal and seasonal variation of convection in the wind-mixed layer of the ocean. *Quart. J. R. Met. Soc.*, **106**, 379–394

1983 'Climatology of the upper boundary layer of the ocean', in *Large-scale oceanographic experiments in the World Climate Research Programme*, Proc. CCCO-JSC Study Conference, Tokyo, May 1982, World Meteorological Organization

1984 'The upper ocean and air–sea interaction in global climate', in *The Global Climate*, (Ed. J. T. Houghton), Cambridge University Press

Woods, J. D. and Onken, R. 1982 Diurnal variation and primary production in the ocean—preliminary results of a Lagrangian ensemble model. *J. Plankton Res.*, **4**, 735–756

Zaneveld, J. R. V. and Spinrad, R. W. 1981 An arctangent model of irradiance in the sea. *J. Geophys. Res.*, **85**, 4919–4922